ARTICLE IN PRESS

S0168-9274(02)00251-9/FLA AID:1427 Vol.●●●(●●●)
ELSGMLTM(APNUM):m2 2003/01/03 Prn:7/01/2003; 13:01
anm1427
P.1 (1-23)
by:violeta p. 1

ELSEVIER

Available at WWW.MATHEMATICSWEB.ORG
POWERED BY SCIENCE DIRECT®

Applied Numerical Mathematics ●●● (●●●●) ●●●–●●●

APPLIED NUMERICAL MATHEMATICS

www.elsevier.com/locate/apnum

A framework for the numerical treatment of aerosol dynamics

Adrian Sandu *, Christian Borden

Department of Computer Science, Michigan Technological University, 1400 Townsend Drive, Houghton, MI 49931, USA

Abstract

This paper presents a general framework for the discretization of particle dynamics equations by projection methods, which include Galerkin and collocation techniques. The framework enables a unified and simultaneous numerical treatment of different dynamic processes like coagulation and growth. Based on the framework a discretization over piecewise polynomial spaces and a spectral discretization are discussed. Numerical examples are given using both linear and logarithmic coordinates.
© 2003 IMACS. Published by Elsevier Science B.V. All rights reserved.

Keywords: Aerosol dynamics; Projection methods; Piecewise polynomials; Spectral approximation

1. Introduction

As our understanding expands, new processes are incorporated into air quality computer models. One example is particulate matter (aerosol) processes, the importance of which is now widely recognized. Aerosols are now a priority focus area in environmental science due to the leading role they play as a cause of adverse human health, and their ability to scatter and absorb incoming solar radiation and thus modify warming due to greenhouse gases and reduce visibility. To accurately study the effects of aerosols it is necessary to resolve aerosol number and mass distributions as a function of chemical composition and size.

In this paper we develop a framework for solving the aerosol dynamics equation, which determines the size distribution of atmospheric particles. Approximations of the size distribution are considered in a suitable finite-dimensional space. The discrete equation is obtained by projecting the dynamics equation onto the discrete space (using a Galerkin or a collocation approach). This approach leads to a bilinear system of coupled ordinary differential equations, which can be solved by a time-stepping method of

* Corresponding author.
E-mail addresses: asandu@mtu.edu (A. Sandu), ctborden@mtu.edu (C. Borden).

0168-9274/03/$30.00 © 2003 IMACS. Published by Elsevier Science B.V. All rights reserved.
doi:10.1016/S0168-9274(02)00251-9

UNCORRECTED PROOF

choice. For simplicity the framework is developed for number densities of single-component particles, but it can be directly extended to mass or volume densities and multiple component particles.

To illustrate the general approach, we consider discretizations over piecewise-polynomial spaces as well a spectral approximation approach, which can also be cast in the proposed framework. A linearly-implicit second order time-stepping method is proposed for the time integration. Numerical examples show that good accuracy is obtained with a relatively small number of grid points.

The paper is organized as follows. Section 2 presents the particle dynamics equations and Section 3 surveys previous efforts to solve these equations numerically. The discretization framework is introduced in Section 4 for number densities; Sections 4.9 and 4.10 present extensions to volume densities and multiple component particles. Section 5 discusses the discretization over piecewise polynomial space and Section 6 discusses the spectral discretization. Numerical results are shown in Section 7, and Section 8 draws conclusions and pinpoints future work.

2. The continuous particle dynamics equation

In this paper continuous particle size distributions are considered functions of particle volume (v) and time (t). The size distribution function (number density) of a family of particles will be denoted by $n(v,t)$; the number of particles per unit volume of air with the volume between v and $v+\mathrm{d}v$ is $n(v,t)\,\mathrm{d}v$. Similar formulations can be given in terms of volume, surface, or mass densities [18]. For simplicity we consider single component particles, but the discretization techniques can be directly generalized to multiple components.

The aerosol population undergoes a series of physical and chemical transformations. *Growth* processes include condensation, evaporation, deposition and sublimation (of gases to/from the particle surface). The growth of each component's volume takes place at a rate that depends on the particle's dimension and composition, $\mathrm{d}v/\mathrm{d}t = I(v)$. *Coagulation* forms new particles of volume $v+w$ from the collision of two smaller particles of volumes v and w; the collision rate $\beta_{v,w}n(v)n(w)$ is proportional to the number of available small particles and to the coagulation kernel $\beta_{v,w}$. *Nucleation* of gases creates small particles. *Emissions* increase the number of particles of a specific composition and size, while *deposition* processes remove particles from the atmosphere. In addition, the constituents interact chemically inside each particle, changing the chemical composition (but not the number) of particles.

Under the above physical transformations the number density changes according to [5]

$$\begin{aligned}\frac{\partial n(v,t)}{\partial t} &= -\partial\big[I(v)\,n(v,t)\big]/\partial v \\ &\quad + \frac{1}{2}\int_0^v \beta_{v-w,w}\,n(v-w,t)n(w,t)\,\mathrm{d}w - n(v,t)\int_0^\infty \beta_{v,w}\,n(w,t)\,\mathrm{d}w \\ &\quad + S(v,t) - R(v,t)\,n(v,t), \\ n(v,0) &= n^0(v), \qquad n(0,t) = 0.\end{aligned} \tag{1}$$

The different terms in Eq. (1) describe, in order, the modification in the number of particles due to growth, creation of particles of volume v by coagulation, loss of volume v particles due to coagulation, increase in particle number due to nucleation, emissions and depositions (sources and sinks). Each of the terms

UNCORRECTED PROOF

will be explained in detail below. The equation is subject to a specified initial condition $n^0(v)$, and the boundary condition of no zero volume particles.

In practice one assumes that the particle population has a nonzero minimal volume and a finite maximal volume, i.e., the dynamic equation is solved on a finite volume interval $[V_{\min}, V_{\max}]$.

$$\begin{aligned}\frac{\partial n(v,t)}{\partial t} &= -\partial\big[I(v)\,n(v,t)\big]/\partial v \\ &\quad + \frac{1}{2}\int_{V_{\min}}^{v-V_{\min}} \beta_{v-w,w}\,n(v-w,t)n(w,t)\,\mathrm{d}w \\ &\quad - n(v,t)\int_{V_{\min}}^{V_{\max}} \beta_{v,w}n(w,t)\,\mathrm{d}w + S(v,t) - R(v,t)n(v,t), \\ n(v,t=0) &= n^0(v), \qquad n(V_{\min},t) = 0.\end{aligned} \tag{2}$$

Note that this equation is no longer self-consistent; for $V_{\min} \leqslant v < 2V_{\min}$ the upper integration limit is smaller than the lower integration limit in the positive coagulation term; we therefore introduce the convention that the positive coagulation term is zero whenever the upper limit is smaller than the lower integration limit.

Particle sizes span orders of magnitude, and to reveal the particle distribution logarithmic coordinates are popular. If we denote

$$x = \log v, \qquad y = \log w, \qquad X_{\min} = \log V_{\min}, \qquad X_{\max} = \log V_{\max},$$

the dynamics equation becomes

$$\begin{aligned}\frac{\partial n(x,t)}{\partial t} &= -e^{-x}\partial\big[I(x)\,n(x,t)\big]/\partial x \\ &\quad + \frac{1}{2}\int_{X_{\min}}^{\log(e^x - e^{X_{\min}})} \beta_{\log(e^x-e^y),y}\,n\big(\log\big(e^x-e^y\big),t\big)n(y,t)e^y\,\mathrm{d}y \\ &\quad - n(x,t)\int_{X_{\min}}^{X_{\max}} \beta_{x,y}\,n(y,t)e^y\,\mathrm{d}w + S(x,t) - R(x,t)n(x,t), \\ n(x,0) &= n^0(x), \qquad n(X_{\min},t) = 0.\end{aligned} \tag{3}$$

3. Previous work

Three major approaches are used to represent the size distribution of aerosols: continuous, discrete and parameterized. In this paper we focus on the numerical approximations of continuous models (i.e., of continuous size distributions and of the general dynamic equations in continuous form).

For computational purposes one needs to use finite-dimensional approximations of the continuous size distributions. In the *sectional approach* the size domain $v \in [0,\infty]$ is divided into size bins $v \in [V_i^{\text{low}}, V_i^{\text{high}})$. In each size bin i there are n_i particles per unit volume, all of them having the

UNCORRECTED PROOF

same mean volume V_i. variations of this approach include the *full-moving* structure, the *quasi-stationary approach*, as well as the *moving-center* structure [10].

A nice survey of several popular numerical methods for particle dynamics equations is given in Zhang et al. [25].

The integro-differential coagulation equation is difficult to solve accurately, due to the fact that the limit of integration of the first term depends on the variable v and the integrands are quadratic (the first term is of nonlinear Volterra type in the terminology of integral equations). The standard discrete version of the coagulation equation uses a monomer size distribution (the volume of the particles in bin each i is a multiple of the smallest volume, $V_i = i\,V_1$, $i = 1, 2, \ldots$). The semi-implicit scheme to solve the discrete coagulation equation [23] is discussed by Jacobson in [10, Section 16]. The differential equation is discretized in time using backward Euler formula, and the quadratic terms $n_{j-\ell}(t)n_\ell(t)$ are replaced by the "linearized" version $n_{j-\ell}(t)n_\ell(t-\Delta t)$, where Δt is the numerical time step size. The scheme can be adapted to general size distributions, and admits a volume-conserving formulation.

A combination of cubic splines (coagulation) and moving finite element techniques (growth part) was used by Tsang and Hippe [24]. Meng, Dabdub and Seinfeld [15] present a size-resolved and chemically-resolved model for aerosol dynamics in a mass density formulation. Gelbard and Seinfeld [5–7] solve the coupled dynamic equations using orthogonal collocation over finite elements. Lushnikov [14] uses generating functions to solve analytically the coagulation equation for particles consisting of monomers of two kinds, under the assumptions of a constant coagulation kernel β and particular initial distributions. Pilinis [18] derives the dynamic equations for multiple component particles and solves the equations using a Galerkin technique with linear elements.

The growth equation in number densities has the form of an advection equation, with the "flow speed" equal to the time derivative of the volume [19, Section 12]. A nice survey of several popular numerical methods for the growth equations is given in Zhang et al. [25]. Different solution methods for the growth equations were proposed in [2,9,12,13]. Dhaniyala and Wexler [4] compare several numerical schemes for modeling aerosol growth. Nguyen and Dabdub [16] use a semi-Lagrangian approach for solving the growth equation.

Many models include different processes successively, using a time splitting scheme. This enables the use of numerical methods tuned to each subprocess but introduces hard-to-quantify splitting errors. A comprehensive discussion is given in Wexler et al. [26]. Simultaneous solutions of all dynamic processes are given in [5–8,15,18,24].

This paper generalizes the previous work of [5–7,18], in that it defines a framework that encompasses both Galerkin and collocation methods and leads to the general form of the discrete equations. Particular discretization methods are built based on the framework formulation using piecewise polynomial elements and spectral elements.

4. A general framework for discretization

We solve Eq. (1) by a semi-discretization in particle size (v), followed by a time integration of the resulting system of ordinary differential equations. The semi-discretization in size is done by projecting the solution on a finite-dimensional subspace $\mathrm{span}\{\phi_1(v), \ldots, \phi_s(v)\}$; this generalizes the sectional approach. The dynamic equation is imposed to hold exactly in a certain subspace (Galerkin approach) or at a certain set of nodes (collocation approach).

UNCORRECTED PROOF

4.1. Discretization of the particle size distribution

The continuous number distribution is given a finite-dimensional approximation. Let $\{\phi_i\}_{1\leqslant i\leqslant s}$ be a set of continuous basis functions; then

$$n(v,t) = \sum_{i=1}^{s} n_i(t)\phi_i(v), \quad \phi_i(v) = \text{basis function}. \tag{4}$$

The set of time-dependent expansion coefficients

$$n(t) = \left[n_1(t), \ldots, n_s(t)\right]^{\mathrm{T}}, \tag{5}$$

will be determined from the dynamics equation.

The representation (4) places the problem in the general framework of *projection methods* [1]. For example ϕ_i can be piecewise polynomials or can be orthogonal polynomials. The result is a continuous distribution $n(v,t)$. Higher order approximations can be obtained by increasing the order of the basis functions without changing the number of bins s.

We note in passing that the full-stationary sectional approach can be formally cast into the form (4) by using Dirac[1] basis functions $\phi_i(v) = \delta(v - V_i)$. For this reason we extend the sectional interpretation and call span$\{\phi_i\}$ the *size bin i*, and refer to n_i as the number of particles in *bin i*.

Logarithmic coordinates. In logarithmic coordinates the basis function arguments are changed accordingly, $\phi_i = \phi_i(x)$.

4.2. Coagulation

The theoretical coagulation equation for single-component particles is [10, Section 16]

$$\frac{\partial n(v,t)}{\partial t} = \frac{1}{2}\int_0^v \beta_{v-w,w} n(v-w,t)n(w,t)\,\mathrm{d}w - n(v,t)\int_0^\infty \beta_{v,w} n(w,t)\,\mathrm{d}w. \tag{6}$$

4.3. The Galerkin approach

To obtain a discrete form of the coagulation equation one inserts (4) into (6):

$$\sum_{i=1}^{s} n_i'(t)\phi_i(v) = \frac{1}{2}\sum_{k=1}^{s}\sum_{m=1}^{s} n_k(t)n_m(t)\int_0^v \beta_{v-w,w}\phi_k(v-w)\phi_m(w)\,\mathrm{d}w - \sum_{k=1}^{s}\sum_{m=1}^{s} n_k(t)n_m(t)\int_0^\infty \beta_{v,w}\phi_k(v)\phi_m(w)\,\mathrm{d}w.$$

[1] Recall that $\delta(x) = 0$ for $x \neq 0$, $\delta(0) = \infty$, and $\int_{V_i-\varepsilon}^{V_i+\varepsilon} f(x)\delta(x - V_i)\,\mathrm{d}x = f(V_i)$.

UNCORRECTED PROOF

Here (and from now on) $n_i'(t)$ denotes the time derivative of $n_i(t)$. The resulting equation is multiplied by the test function $\xi_j(v)$ $(j = 1, \ldots, s)$ and integrated from $v = 0$ to ∞ to obtain a system of s ordinary differential equations

$$\begin{aligned}
&\sum_{i=1}^{s} n_i'(t) \int_0^\infty \phi_i(v)\xi_j(v)\,\mathrm{d}v \\
&\quad = \frac{1}{2}\sum_{k=1}^{s}\sum_{m=1}^{s} n_k(t)n_m(t) \int_0^\infty \left(\int_0^v \beta_{v-w,w}\phi_k(v-w)\phi_m(w)\,\mathrm{d}w \right) \xi_j(v)\,\mathrm{d}v \\
&\quad\quad - \sum_{k=1}^{s}\sum_{m=1}^{s} n_k(t)n_m(t) \int_0^\infty \left(\int_0^\infty \beta_{v,w}\phi_m(w)\,\mathrm{d}w \right) \phi_k(v)\xi_j(v)\,\mathrm{d}v. \qquad (7)
\end{aligned}$$

We build the following matrices of integral coefficients

$$\begin{aligned}
A &= \left[\int_0^\infty \phi_j(v)\xi_i(v)\,\mathrm{d}v \right]_{1\leqslant i,j\leqslant s}, \\
B^j &= \left[\frac{1}{2} \int_0^\infty \left(\int_0^v \beta_{v-w,w}\phi_k(v-w)\phi_m(w)\,\mathrm{d}w \right) \xi_j(v)\,\mathrm{d}v \right]_{1\leqslant k,m\leqslant s}, \qquad (8) \\
C^j &= \left[\int_0^\infty \left(\int_0^\infty \beta_{v,w}\phi_m(w)\,\mathrm{d}w \right) \phi_k(v)\xi_j(v)\,\mathrm{d}v \right]_{1\leqslant k,m\leqslant s}, \quad 1 \leqslant j \leqslant s.
\end{aligned}$$

If $n(t)$ is the vector of number concentrations (5), Eq. (7) becomes

$$An'(t) = \begin{bmatrix} n^{\mathrm{T}}(t)(B^1 - C^1)n(t) \\ \vdots \\ n^{\mathrm{T}}(t)(B^s - C^s)n(t) \end{bmatrix}. \qquad (9)$$

One can regard B and C as 3-tensors, in which case the semi-discrete coagulation equation reads

$$An'(t) = \big[(B - C) \times n(t)\big] \cdot n(t). \qquad (10)$$

In the pure *Galerkin* approach [1] $\{\phi_i(v)\} = \{\xi_i(v)\}$ are (piecewise) continuous basis functions. Eq. (9) is relatively expensive to solve, since one has to evaluate a large number of double integrals for building the tensors B and C. If $\beta(v, w)$ does not change in time one can compute the tensors once and reuse them throughout integration, thus making the whole process computationally feasible.

UNCORRECTED PROOF

Logarithmic coordinates. In logarithmic coordinates the coagulation tensor entries become

$$B^j_{k,m} = \frac{1}{2}\int_{X_{\min}}^{X_{\max}} \xi_j(x) \int_{X_{\min}}^{\log(e^x - e^{X_{\min}})} \beta_{z,y}\phi_k(z)\phi_m(y)e^y \,\mathrm{d}y\,\mathrm{d}x,$$
$$\text{where } z(x,y) = \log\left(e^x - e^y\right), \tag{11}$$
$$C^j_{k,m} = \int_{X_{\min}}^{X_{\max}} \phi_k(x)\xi_j(x) \int_{X_{\min}}^{X_{\max}} \beta_{x,y}\phi_m(y)e^y \,\mathrm{d}y\,\mathrm{d}x.$$

4.4. The collocation approach

In the *collocation* approach $\{\phi_i(v)\}$ are continuous basis functions, but the test functions are deltas, $\{\xi_i(v) = \delta(v - V_i^c)\}$, with V_i^c the collocation points. The resulting equation is also of form (9), but the integral coefficients to be computed simplify to

$$A = \left[\phi_j\left(V_i^c\right)\right]_{1\leqslant i,j\leqslant s},$$
$$B^j = \left[\frac{1}{2}\int_0^v \beta_{V_j^c - w,w}\phi_k\left(V_j^c - w\right)\phi_m(w)\,\mathrm{d}w\right]_{1\leqslant k,m\leqslant s}, \quad 1 \leqslant j \leqslant s, \tag{12}$$
$$C^j = \left[\phi_k\left(V_j^c\right)\int_0^\infty \beta_{V_j^c,w}\phi_m(w)\,\mathrm{d}w\right]_{1\leqslant k,m\leqslant s}, \quad 1 \leqslant j \leqslant s.$$

This approach is computationally less expensive since all coefficients involve only simple integrals. Note that if the basis functions have the interpolation property $\phi_i(V_j) = 0$ for $i \neq j$ and $\phi_i(V_i) = 1$ then the "mass matrix" A is the unit matrix.

Logarithmic coordinates. In logarithmic coordinates the tensor entries are

$$B^j_{k,m} = \frac{1}{2}\int_{X_{\min}}^{\log(e^{X_j^c} - e^{X_{\min}})} \beta_{\log(e^{X_j^c} - e^y),y}\phi_k\left(\log\left(e^{X_j^c} - e^y\right)\right)\phi_m(y)e^y\,\mathrm{d}y,$$
$$C^j_{k,m} = \phi_k\left(X_j^c\right)\int_{X_{\min}}^{X_{\max}} \beta_{X_j^c,y}\phi_m(y)e^y\,\mathrm{d}y. \tag{13}$$

A note on the coagulation kernel. The coagulation kernel $\beta_{v,w}$ is usually assumed to depend only on particle size (but be time-independent on large time periods and concentration-independent). With this assumption the discretization three-tensors can be computed only once, and then used throughout the simulation, which leads to considerable computational savings. If the coagulation kernel changes in time $\beta_{v,w}(t)$ then the tensors will need to be recomputed periodically (e.g., at each update of the meteorological fields). Finally, if the kernel depends on the chemical composition of the particles then the tensors need to be recomputed at each time step.

UNCORRECTED PROOF

ARTICLE IN PRESS

S0168-9274(02)00251-9/FLA AID:1427 Vol.●●●(●●●)
ELSGMLTM(APNUM):m2 2003/01/03 Prn:7/01/2003; 13:01
anm1427
P.8 (1-23)
by:violeta p. 8

4.5. Growth

Growth processes include condensation, evaporation, deposition and sublimation (of gases to/from the particle surface). Consider again the case of single component particles. The growth equation in number densities

$$\frac{\partial n(v,t)}{\partial t} = -\frac{\partial}{\partial v}\big[I(v)n(v,t)\big], \quad I(v) = \frac{\mathrm{d}v(t)}{\mathrm{d}t}, \tag{14}$$

$$n(0,t) = 0, \quad n(v,0) = n^0(v), \tag{15}$$

has the form of an advection equation, with the "flow speed" provided by the time derivative of the volume. This equation is to be solved subject to an initial distribution $n^0(v)$ and the boundary condition of no zero-sized particles [19, Section 12],

A similar derivation process (as presented for coagulation) leads to the semi-discrete formulation of the growth equations

$$An'(t) = Gn(t), \tag{16}$$

where

$$A = \left[\int_0^\infty \phi_j(v)\xi_i(v)\,\mathrm{d}v\right]_{1\leqslant i,j\leqslant s}, \qquad G = \left[\int_0^\infty I(v)\phi_j(v)\xi_i'(v)\,\mathrm{d}v\right]_{1\leqslant i,j\leqslant s}. \tag{17}$$

For G we have used one integration by parts and homogeneous boundary conditions at $v = 0$ and $v = \infty$. For the Galerkin approach use $\xi_i = \phi_i$. For the collocation approach one obtains

$$A = \big[\phi_j\big(V_i^{\mathrm{c}}\big)\big]_{1\leqslant i,j\leqslant s}, \qquad G = \left[-\frac{\mathrm{d}[I\phi_j]}{\mathrm{d}v}\big(V_i^{\mathrm{c}}\big)\right]_{1\leqslant i,j\leqslant s}. \tag{18}$$

Logarithmic coordinates. In the logarithmic Galerkin formulation (3) the matrix entries read

$$A_{i,j} = \int_{X_{\min}}^{X_{\max}} \phi_j(x)\phi_i(x)\,\mathrm{d}x, \qquad G_{i,j} = \int_{X_{\min}}^{X_{\max}} \frac{\mathrm{d}}{\mathrm{d}x} I(x)\phi_j(x)\frac{\mathrm{d}}{\mathrm{d}x}\big(e^{-x}\xi_i'(x)\big)\mathrm{d}x \tag{19}$$

while for the logarithmic collocation they are

$$A_{i,j} = \phi_j\big(X_i^{\mathrm{c}}\big), \qquad G_{i,j} = -e^{-X_i^{\mathrm{c}}}\frac{\mathrm{d}[I\phi_j]}{\mathrm{d}x}\big(X_i^{\mathrm{c}}\big). \tag{20}$$

4.6. Sources and sinks

Sources and sinks (i.e., emissions, nucleation and deposition processes) have a simple mathematical formulation,

$$\frac{\partial n(v,t)}{\partial t} = S(v,t) - R(v,t)n(v,t). \tag{21}$$

UNCORRECTED PROOF

The simplicity comes from the fact that S and R terms are not coupled across different volumes; finite-dimensional approximations of these terms can be given

$$S(v,t) = \sum_{i=1}^{s} S_i(t)\phi_i(v), \qquad R(v,t) = \sum_{i=1}^{s} R_i(t)\phi_i(v),$$

which leads to the discrete evolution equation

$$n'(t) = S(t) - R(t)n(t), \tag{22}$$

where

$$S(t) = \big[S_1(t), \ldots, S_s(t)\big]^{\mathrm{T}} \quad \text{and} \quad R(t) = \operatorname{diag}\big[R_1(t), \ldots, R_s(t)\big].$$

4.7. Simultaneous discretization of the dynamic equations

Of particular interest is the coupled solution of coagulation, growth, nucleation, emissions and deposition. The coupled approach will, for example, better capture the competition between nucleation of new particles and condensation on existing particles for gas-to-particle conversion [25].

For single component particles combining (9), (16) and (22) gives the semi-discrete aerosol dynamics equation

$$An'(t) = \underbrace{Gn(t)}_{\text{growth}} + \underbrace{\big[(B-C)\times n(t)\big]n(t)}_{\text{coagulation}} + \underbrace{AS(t)}_{\text{sources}} - \underbrace{AR(t)n(t)}_{\text{deposition}}. \tag{23}$$

This is a system of s coupled ordinary differential equations. The discrete initial conditions

$$n(0) = n^0 \tag{24}$$

are derived by projecting the continuous initial distribution $n_0(v)$ onto the finite-dimensional solution space,

$$n^0(v) = \sum_{i=1}^{s} n_i^0 \phi_i(v), \qquad n^0 = \big[n_1^0, \ldots, n_s^0\big]^{\mathrm{T}}.$$

4.8. Time integration

The system (23), (24) can be solved by any appropriate time-stepping method. The system has a particular form: the growth term is linear, while the coagulation term is bilinear. This makes it easy to express the Jacobian for implicit methods.

Particularly attractive are linearized versions of the implicit numerical methods which avoid iterative solutions. The following linearized backward Euler time discretization has second order time accuracy for the coagulation term:

$$An\big(t^{k+1}\big) = An\big(t^k\big) + \frac{\Delta t}{2} J^{\mathrm{coag}}\big(n\big(t^k\big)\big) n\big(t^{k+1}\big), \tag{25}$$

where the Jacobian of the coagulation term is

$$J^{\mathrm{coag}}(n) = \begin{bmatrix} n^{\mathrm{T}} D^1 \\ \vdots \\ n^{\mathrm{T}} D^s \end{bmatrix}, \qquad D^i = \big(B^i - C^i\big) + \big(B^i - C^i\big)^{\mathrm{T}}, \quad 1 \leqslant i \leqslant s. \tag{26}$$

UNCORRECTED PROOF

This can be coupled with the Crank–Nicholson method for the growth and source terms to obtain the second order, non-iterative scheme

$$\left(A - \frac{\Delta t}{2}\left[J^{\text{coag}}\left(n\left(t^k\right)\right) + G + AR\left(t^{k+1}\right)\right]\right)n\left(t^{k+1}\right) = \left(A + \frac{\Delta t}{2}\left[G + AR\left(t^k\right)\right]\right)n\left(t^k\right) + \frac{\Delta t}{2}\left[S\left(t^{k+1}\right) + S\left(t^k\right)\right]. \tag{27}$$

4.9. Extension to volume densities

The framework can be easily extended to treat volume, surface, or mass densities. For example, the volume density $\mathsf{V}(v,t) = vn(v,t)$ can be discretized as

$$\mathsf{V}(v,t) = \sum_{i=1}^{s} \mathsf{V}_i(t)\phi_i(v).$$

The aerosol dynamics equation for volume densities is

$$\begin{aligned}
&\partial \mathsf{V}(v,t)/\partial t \\
&\quad = -\partial\left[\mathsf{V}(v,t)I(v)\right]/\partial v + \mathsf{V}(v,t)I(v)/v \quad \text{(growth)} \\
&\qquad + \int_0^v \frac{\beta_{v-w,w}}{w}\mathsf{V}(v-w,t)\mathsf{V}(w,t)\,\mathrm{d}w \quad \text{(coagulation)} \\
&\qquad - \mathsf{V}(v,t)\int_0^\infty \frac{\beta_{v,w}}{w}\mathsf{V}(w,t)\,\mathrm{d}w \\
&\qquad + S(v,t) - R(v,t)\mathsf{V}(v,t) \quad \text{(sources, deposition)}.
\end{aligned} \tag{28}$$

A discretization of Eq. (28) can be obtained following the framework approach; one obtains a discrete system of the form (27) with B, C and G redefined accordingly.

4.10. Extension to multiple components

Complex models treat particles composed of multiple chemical constituents. Let $v_q(v,t)$, $q = 1,\ldots,m$ be the volume of the qth chemical component in particles of volume v; the multi-component aerosol population is described by the individual volume densities of each constituent $\mathsf{V}^q(v,t) = v_q(v,t)n(v,t)$; the total volume of component q (per unit volume of air) contained in all particles having individual volumes between v and $v + \mathrm{d}v$ is $\mathsf{V}^q(v,t)\,\mathrm{d}v$. Under these transformations the volume densities of each constituent $\mathsf{V}^q(v,t)$, $q = 1,\ldots,m$ change according to [5,18]

$$\begin{aligned}
&\partial \mathsf{V}^q(v,t)/\partial t \\
&\quad = -\partial\left[\mathsf{V}^q(v,t)\sum_{k=1}^{m} I_k(v)\right]/\partial v + \mathsf{V}(v,t)I_q(v)/v \quad \text{(growth)}
\end{aligned}$$

UNCORRECTED PROOF

$$
\begin{aligned}
&+ \int_0^v \frac{\beta_{v-w,w}}{w} \mathsf{V}^q(v-w,t)\mathsf{V}(w,t)\,\mathrm{d}w \quad \text{(coagulation)}\\
&- \mathsf{V}^q(v,t) \int_0^\infty \frac{\beta_{v,w}}{w} \mathsf{V}(w,t)\,\mathrm{d}w\\
&+ S_q(v,t) \quad \text{(sources)}\\
&- R_q(v,t)\mathsf{V}^q(v,t) \quad \text{(deposition)}\\
&+ K\left(\mathsf{V}^1,\ldots,\mathsf{V}^m,t\right), \quad q=1,\ldots,m \quad \text{(chemistry)}
\end{aligned} \tag{29}
$$

where $\mathsf{V}(v,t)=\sum_{q=1}^m \mathsf{V}^q(v,t)$ is the total volume distribution; the m integro-differential equations are coupled through $\mathsf{V}(v,t)$ and $K(\mathsf{V}^1,\ldots,\mathsf{V}^m,t)$. The system (29) is subject to the initial and boundary conditions

$$
\mathsf{V}^q(v,t=0)=\left(\mathsf{V}^q\right)^0(v), \quad \mathsf{V}^q(v=0,t)=0, \quad q=1,\ldots,m. \tag{30}
$$

Eqs. (29), (30) can be discretized in size using the same approach. For each component volume one has

$$
\mathsf{V}^q(v,t)=\sum_{i=1}^s \mathsf{V}_i^q(t)\phi_i(v), \quad \mathsf{V}_i^q(t)=\mathsf{V}^q(V_i,t), \quad q=1,\ldots,m, \tag{31}
$$

and the semidiscrete system reads

$$
\begin{aligned}
\frac{\mathrm{d}}{\mathrm{d}t}\mathsf{V}^q(t) \;=\; & \underbrace{G\mathsf{V}^q(t)+\mathrm{diag}_{1\leqslant i\leqslant s}\left(\frac{I_q(V_i)}{V_i}\right)\cdot\sum_{k=1}^m \mathsf{V}^k(t)}_{\text{growth}}\\
& + \underbrace{\left[(B-C)\times\sum_{k=1}^m \mathsf{V}^k(t)\right]\cdot\mathsf{V}^q(t)}_{\text{coagulation}}\\
& + \underbrace{S(t)}_{\text{nucl.+em}} - \underbrace{R_q\mathsf{V}^q(t)}_{\text{dep.}} + \underbrace{K\left(\mathsf{V}^1,\ldots,\mathsf{V}^m,t\right)}_{\text{chem.}}, \quad q=1,\ldots,m.
\end{aligned}
$$

The matrix G and the tensors B and C are redefined according to (29). Note that the same G, B, C are used for all chemical components q, which makes the method efficient.

5. Piecewise-polynomial discretization

Consider now the discrete space of piecewise-polynomials of order smaller than or equal to r, $P_r(V_{\min}, V_{\max})$. We assume that $s-1$ is a multiple of r; the functions are polynomial on each interval $[V_{1+\ell r}, V_{1+(\ell+1)r}]$. A basis of P_r is provided by the Lagrange polynomials in each interval, with the

UNCORRECTED PROOF

$r+1$ nodes given by $V_{1+\ell r}, V_{2+\ell r}, \ldots, V_{1+r+\ell r}$. Thus, the basis functions ϕ_i have compact support, are piecewise-polynomials of order less than or equal to r and satisfy the relation

$$\phi_i(V_j) = \begin{cases} 1, & \text{for } i = j, \\ 0, & \text{for } i \neq j. \end{cases}$$

The discrete approximation

$$n(v,t) = \sum_{i=1}^{s} n(V_i,t)\phi_i(v) = \sum_{i=1}^{s} n_i(t)\phi_i(v)$$

is the order r piecewise-polynomial interpolant of $n(v,t)$ with nodes V_i. Let $h = \max_i |V_{i+1} - V_i|$. Assuming smooth solutions $n(v,t)$ the interpolation order is

$$\left| n(v,t) - \sum_{i=1}^{s} n(V_i,t)\phi_i(v) \right| = \mathrm{O}\big(h^{r+1}\big).$$

In general one expects that the approximation order is given by the interpolation order.

A direct approach is to consider the system as being discretized first in time then in size. The time integration method (25) applied to the coagulation system leads to the linear second order Fredholm equation (with unknown function $n(v,t^{k+1})$)

$$\begin{aligned} n\big(v,t^{k+1}\big) = n\big(v,t^k\big) &+ \frac{\Delta t}{2}\int_0^v \frac{\beta_{v-w,w} + \beta_{w,v-w}}{2} n\big(v-w,t^k\big) n\big(w,t^{k+1}\big)\,\mathrm{d}w \\ &- \frac{\Delta t}{2} n\big(v,t^{k+1}\big)\int_0^\infty \beta_{v,w} n\big(w,t^k\big)\,\mathrm{d}w \\ &- \frac{\Delta t}{2} n\big(v,t^k\big)\int_0^\infty \beta_{w,v} n\big(w,t^{k+1}\big)\,\mathrm{d}w. \end{aligned} \tag{32}$$

The Galerkin or collocation discretization over $P_r(V_{\min}, V_{\max})$ compute a solution which approximates $n(v,t^{k+1})$ with an accuracy of $\mathrm{O}(h^{r+1})$ [1, Section 3.1.3].

In practice the observed convergence orders may be faster than this theoretical bound ("superconvergence"), especially if one considers node point values. For example, the collocation method approximates

$$\begin{aligned} n\big(V_j^c,t\big)\int_0^\infty \beta_{V_j^c,w} n(w,t)\,\mathrm{d}w &\approx \sum_{k,m=1}^{s} n_k(t) n_m(t) C_{k,m}^j \\ &= \left(\sum_{k=1}^{s} n_k(t)\phi_k\big(V_j^{\mathrm{c}}\big)\right)\int_0^\infty \beta_{V_j^{\mathrm{c}},w}\left(\sum_{m=1}^{s} n_m(t)\phi_m(w)\right)\mathrm{d}w. \end{aligned}$$

If the collocation points are the node points $V_j^{\mathrm{c}} = V_j$ then $n(V_j,t) = \sum_{k=1}^{s} n_k(t)\phi_k(V_j)$ by the interpolation requirement. For smooth β the term $\int_0^\infty \beta_{V_j^{\mathrm{c}},w}(\sum_{m=1}^{s} n_m(t)\phi_m(w)\,\mathrm{d}w)$ is a weighted Newton–Cotes approach for integration, therefore if r is even the negative term is approximated within

UNCORRECTED PROOF

$O(h^{r+2})$. However, this does not hold for the positive coagulation term (consider, for example, the case $j = 1$).

The collocation method is less expensive computationally and provides the same order of accuracy, so in principle it is to be preferred. Note at this point that if the collocation points are the node points then the mass matrix A is the identity matrix, and the tensor C is 2-dimensional,

$$C^j = \left[\delta_{k,j} \int_0^\infty \beta_{V_j^c,w} \phi_m(w)\, \mathrm{d}w \right]_{1 \leqslant k,m \leqslant s}, \quad 1 \leqslant j \leqslant s.$$

The order of accuracy shows how to carry out the numerical evaluation of integral coefficients. If B, C are approximated within $O(h^{r+1})$ the order of accuracy remains unchanged, and if the integral coefficients are approximated within $O(h^{r+2})$ the integration errors become negligible when compared to discretization errors for small h. One can use a Gaussian quadrature with $(r+1) \div 2$ nodes.

The pure Galerkin approximation of the growth term is accurate to order $O(h^r)$ [11, Section 9.3]. Note that an upwind Petrov–Galerkin method is more appropriate to ensure stability of the hyperbolic growth term, in which case the order of approximation may be $O(h^{r+0.5})$; a discussion is outside the scope of this paper. The collocation method for piecewise polynomial basis functions cannot be directly extended to the growth term due to non-differentiability at node points (which were chosen to be the collocation points also).

This discussion leads to the following idea for an $O(h^{r+1})$ discretization of the coagulation-growth equation. Discretize the coagulation term using collocation on P_r and use a Galerkin approximation on P_{r+1} for the growth term. Replace the integrals by repeated $[r/2]$-point Gaussian quadrature on each $[V_i, V_{i+1}]$ subinterval. Matrices A and G are then defined using the basis polynomials of P_{r+1}, while the tensors B and C are computed from the basis functions of P_r. Using the timestepping formula (27) the combined numerical method for coagulation-growth can be written as

$$\left(A - \frac{\Delta t}{2} A J^{\mathrm{coag}}\big(n(t^k)\big) - \frac{\Delta t}{2} G \right) n(t^{k+1}) = \left(A + \frac{\Delta t}{2} G \right) n(t^k).$$

6. Spectral discretization

In this section we review some important aspects of spectral interpolation. Consider the set of s Chebyshev points in the interval $[V_{\min}, V_{\max}]$ (cf. [22])

$$V_j = V_{\min} + \frac{V_{\max} - V_{\min}}{2} \left[1 - \cos\left(\frac{j-1}{s-1} \pi \right) \right], \quad j = 1, \ldots, s. \tag{33}$$

Let $f(v)$ be a function on $v \in [V_{\min}, V_{\max}]$, and $p(v)$ the unique interpolation polynomial of degree at most $s-1$ such that

$$p(V_j) = f(V_j), \quad j = 1, \ldots, s.$$

The polynomial can be expressed in terms of the Lagrange basis functions associated with the Chebyshev set of points (33); then

$$p(v) = \sum_{i=1}^{s} f(V_i) \mathsf{L}_i(v), \quad \mathsf{L}_i(v) = \frac{\prod_{k \neq i} (v - V_k)}{\prod_{k \neq i} (V_i - V_k)} \quad \text{for all } i. \tag{34}$$

UNCORRECTED PROOF

This polynomial is a very accurate approximate of f. We recall the following result from Trefethen [22, Chapter 5]; for more details the reader is invited to consult Trefethen's book.

Accuracy of spectral polynomial interpolation. If $f(v)$ is smooth enough[2] there exist $C_1, C_2 > 0$ (independent of s) such that the interpolation error is

$$\left|f(v) - p(v)\right| \leqslant C_1 e^{-C_2 s}, \quad \text{for all } v \in [V_{\min}, V_{\max}]. \tag{35}$$

This is called "spectral accuracy".

Moreover, at the interpolation points the derivative of p is a good approximation of the derivative of f, more exactly there exist $C_3, C_4 > 0$ (independent of s)

$$\left|\frac{\partial f}{\partial v}(V_j) - \frac{\partial p}{\partial v}(V_j)\right| \leqslant C_3 e^{-C_4 s}, \quad \text{for all } j = 1, \ldots, s.$$

The derivative of p at the interpolation points can be easily computed with the help of the Chebyshev differentiation matrix D_s [22, Chapter 6]

$$\begin{bmatrix} \frac{\partial p}{\partial v}(V_1) \\ \vdots \\ \frac{\partial p}{\partial v}(V_s) \end{bmatrix} = -\frac{2}{V_{\max} - V_{\min}} D_s \cdot \begin{bmatrix} p(V_1) \\ \vdots \\ p(V_s) \end{bmatrix}, \tag{36}$$

where

$$(D_s)_{ij} = \begin{cases} \frac{2(s-1)^2}{6} & i = j = 1, \\ 2\frac{(-1)^{i+j}}{V_i - V_j} & i = 1, 1 < j \leqslant s, \\ -\frac{(-1)^{i+j}}{V_i - V_j} & 1 < i \neq j < s, \\ -\frac{V_j}{2(1-V_j^2)} & 1 < i = j < s, \\ \frac{(-1)^{i+j}}{V_i - V_j} & 1 < i \neq j < s, \\ \frac{(-1)^{i+j}}{2(V_i - V_j)} & j = 1, 1 < i \leqslant s, \\ -\frac{2(s-1)^2}{6} & i = j = s. \end{cases}$$

Consequently, the function derivative at the node points can be approximated with spectral accuracy by $[\partial f/\partial v(V_i)]_{1 \leqslant i \leqslant s} \approx D_s \cdot [f(V_i)]_{1 \leqslant i \leqslant s}$.

A spectral discretization of (1) consists in replacing the continuous density function $n(v, t)$ by its spectral interpolation polynomial; the framework discrete formulation (23) then holds with the basis functions given by the Lagrange polynomials (34)

$$\phi_i(v) = \mathsf{L}_i(v), \quad i = 1, \ldots, s.$$

[2] Analytic in an elliptic region in the complex plane that contains the interval $[V_{\min}, V_{\max}]$.

UNCORRECTED PROOF

7. Numerical experiments

7.1. Test problem I

For the numerical experiments we first consider the test problem from Gelbard and Seinfeld [6]. Let N_t be the total initial number of particles and V_m the mean initial volume. The initial number distribution is exponential, the coagulation rate is constant, and the growth rate is linear with the volume:

$$N_t(v) = (N_t/V_m)e^{-v/V_m}, \qquad \beta(v,w) = \beta_o, \qquad I(v) = \sigma_o v.$$

This test problem admits the analytical solution [6]

$$n^A(v,t) = \frac{4N_t}{V_m(N_t\beta_o t+2)^2}\cdot\exp\left(\frac{-2v\exp(\sigma_o t)}{V_m(N_t\beta_o t+2)} - \sigma_o t\right). \tag{37}$$

We consider the values $\beta_o = 2.166\times10^{-6}$ cm^3 hour^{-1} particles^{-1}, $\sigma_o = 0.03$ hour^{-1}, $N_t = 10^4$ particles, $V_m = 0.03$ μm^3.

The distribution is truncated to the volume interval $V_{\min} = 0$ μm^3, $V_{\max} = \pi/6$ μm^3. The node points are uniformly spaced for the piecewise-polynomial experiment, and located at the Chebyshev points for the spectral approximation. We solve the dynamics equation in the time interval $[t_0 = 0, t_{\text{final}} = 6]$ hours with the very small time step Δt = 1 second.

Tests were performed for coagulation-only ($\sigma_o = 0$), growth-only ($\beta_o = 0$), and combined coagulation-growth problems. The solution errors at the end of the simulation interval were measured by the root mean square (RMS) norm at the node points

$$Err = \sqrt{\frac{1}{s}\sum_{i=1}^{s}\frac{[n_i(t_{\text{final}}) - n^A(V_i,t_{\text{final}})]^2}{\max(n^A(V_i,t_{\text{final}}),\text{Thr})^2}},$$

where n is the numerical solution, n^A the analytical solution, and the threshold Thr = 1000 particles cm^{-3} μm^{-3}.

The discretization errors versus the number of bins are presented in Fig. 1 and the experimental convergence orders in Table 1. For coagulation the experimental order of convergence of piecewise polynomial elements is $r+1$ for odd r and $r+2$ for even r, which is similar to Newton–Cotes quadrature convergence order. For comparison we include the classical semi-implicit method [10, Section 16]; it shows second order behavior. The spectral method converges faster than any order (spectral convergence). For growth and combined coagulation-growth the convergence orders are $r+1$ for the linear and quadratic elements; $r+2$ for fourth order elements; the spectral method displays exponential convergence. The experimental orders for piecewise polynomial elements are better than predicted, showing superconvergence at the grid points.

7.2. Test problem II

Problem II is the exponential test problem solved in the logarithmic formulation (3). The distribution is truncated to the volume interval $V_{\min} = \pi/6\times10^{-9}$ μm^3, $V_{\max} = \pi/6$ μm^3. The node points are log-uniformly spaced for the piecewise-polynomial experiment, and located at the log-Chebyshev points in the logarithmic volume interval for the spectral approximation.

UNCORRECTED PROOF

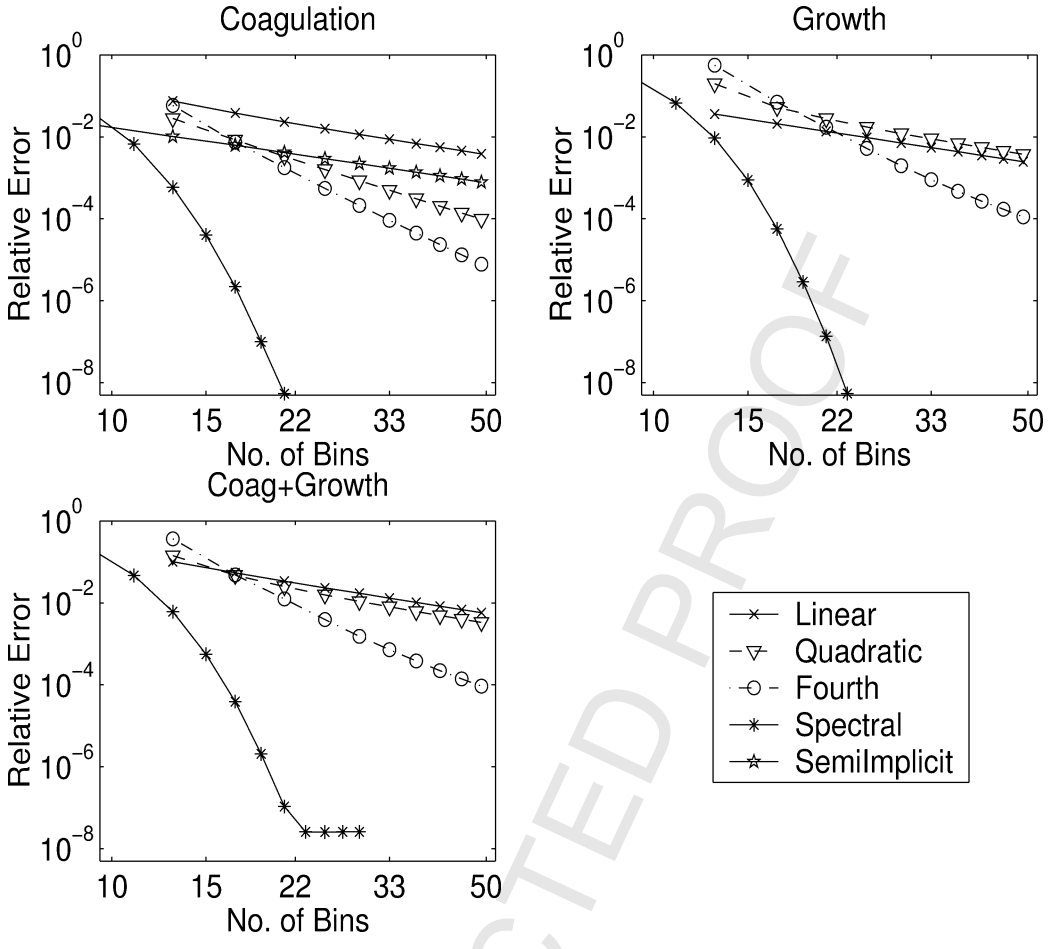

Fig. 1. Solution RMS errors at $t_{\text{final}} = 6$ hours for test problem I.

Table 1
Experimental orders of convergence for different methods and test problems. C and G stand for coagulation and growth, respectively

	Test I			Test II			Test III		
	C	G	C+G	C	G	C+G	C	G	C+G
Linear	2.22	2.02	2.14	2.04	4.21	1.96	2.04	2.14	2.04
Quadr.	4.25	2.81	2.72	3.85	2.23	2.39	3.30	1.87	1.97
Fourth	6.64	6.39	6.20	3.40	4.59	4.13	3.14	2.20	2.19
Spectral	exp	exp	exp	exp	exp	exp	3.76	2.90	1.87
Semiimp.	1.93	–	–	1.83	–	–	1.81	–	–

The discretization errors versus the number of bins are presented in Fig. 2. More bins are needed in logarithmic coordinates than in linear coordinates for a similar accuracy (note the scales of the axes compared to linear coordinates results). The experimental orders of convergence are shown in

UNCORRECTED PROOF

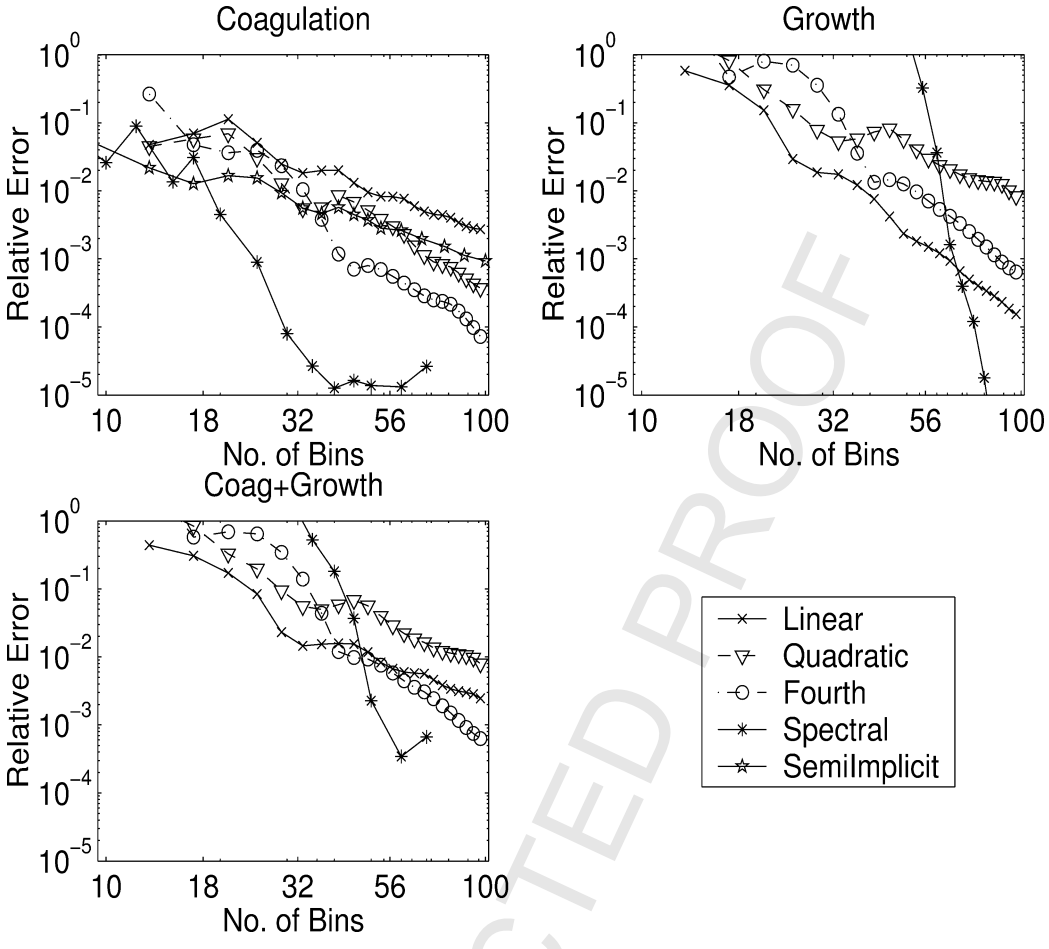

Fig. 2. Solution RMS errors at $t_{\text{final}} = 6$ hours for test problem II.

Table 1. Linear elements show better than expected convergence for growth; and second order behavior for coagulation and the complete test problem. Quadratic elements show fourth order behavior for coagulation (see Newton–Cotes quadrature) and second order for growth and complete. Fourth order elements have a less than expected order for coagulation but display fourth order convergence for growth and combined. Spectral discretization shows spectral convergence, while the semi-implicit method displays second order behavior.

7.3. *Test problem III*

We now consider a second test problem that is posed in naturally logarithmic coordinates. Here $\beta_o = 1.083 \times 10^{-3}$ cm^3 hour^{-1} particles^{-1}, $I(v) = \sigma_o v$ with $\sigma_o = 0.2$ hour^{-1}, and $N_t = 10^4$ particles. The volume interval is $V_{\min} = 10^{-3}$ μm^3, $V_{\max} = 1$ μm^3, the time interval $t_0 = 0$, $t_{\text{final}} = 1$ hour, and the time step $\Delta t = 1$ second.

UNCORRECTED PROOF

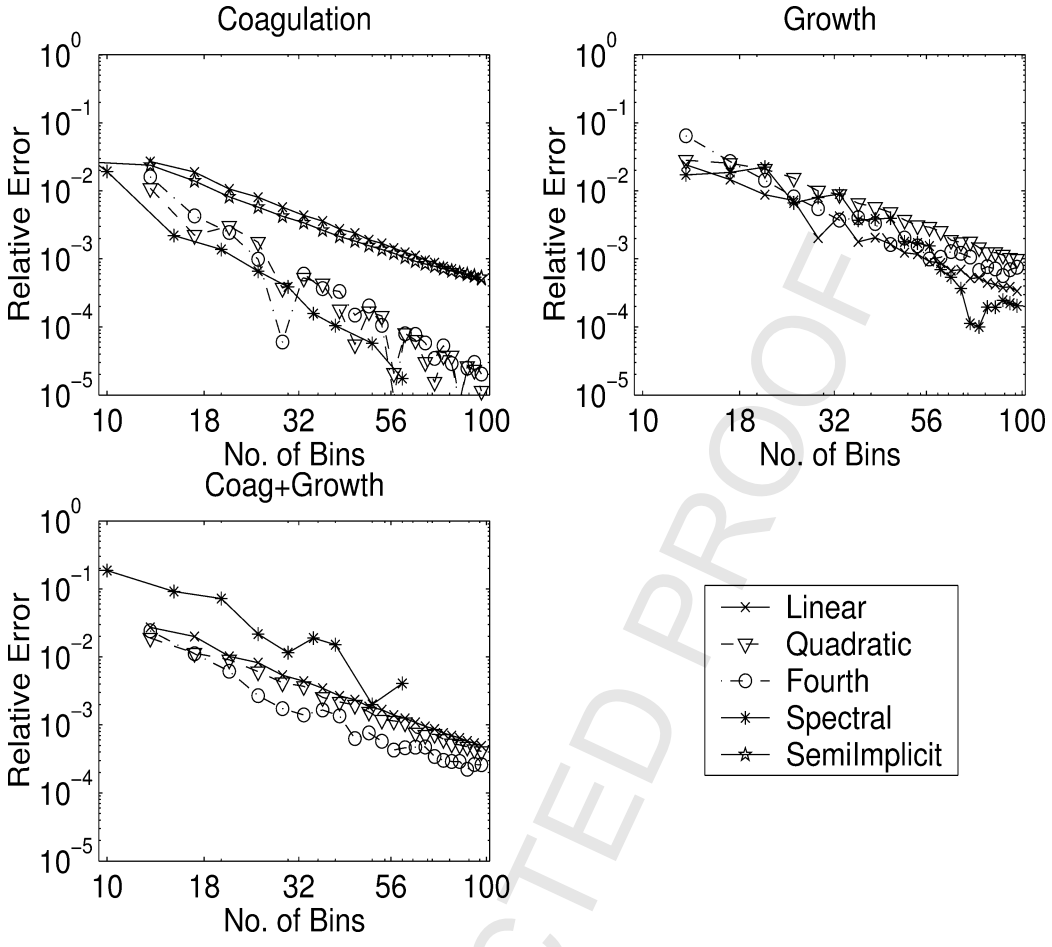

Fig. 3. Solution RMS errors at $t_{\text{final}} = 1$ hour for test problem III.

The initial concentration is a cosine hill in logarithmic coordinates

$$n_0(v) = \begin{cases} \frac{N_t}{2} \cdot \left[1 - \cos\left(2\pi \frac{\log v - x_{\min}}{x_{\max} - x_{\min}}\right)\right], & x_{\min} < \log v < x_{\max}, \\ 0, & \log v \leqslant x_{\min} \text{ or } \log v \geqslant x_{\max}. \end{cases}$$

The limits $x_{\min}$ and $x_{\max}$ define the support of the initial concentration and are such that

$$\log V_{\min} < x_{\min} < x_{\max} < \log V_{\max}.$$

No analytical solution is available. A reference solution was obtained using the semi-implicit method for coagulation [10] on the uniform grid $V_i = i \cdot \Delta v$, $\Delta v = 10^{-4}$ μm^3, such that $V_1 = V_{\min}$ and $V_{10,000} = V_{\max}$; the first order upwinding scheme was employed for the discretization of the growth term. Fig. 4 shows the initial distribution, as well as the coagulation-growth solution after 1 hour.

For the numerical solutions we use log-uniform grids for the piecewise-polynomial experiment, and log-Chebyshev grids for the spectral approximation. Fig. 3 displays the numerical errors. The experimental convergence orders for coagulation are between 2 (linear, semi-implicit) and 3 (quadratic and fourth order). The growth results show (nearly) second order convergence for all element types.

UNCORRECTED PROOF

The spectral discretization does not display spectral convergence; this is presumably due to the limited smoothness of the profile (e.g., the second derivative of the initial profile is not continuous). A more detailed analysis is needed to explain why the experimental convergence orders for piecewise polynomial elements are smaller than the polynomial orders.

The results presented so far indicate that the growth problem in logarithmic coordinates is more challenging than coagulation; and requires more bins for similar accuracy. The direct approach is to increase the number of bins such that the appropriate resolution is obtained for growth; however the cost of building the tensors for coagulation becomes significant.

In order to avoid these extra costs we propose the following approach, based on different grids for coagulation and for growth. Let $\{x_i\}$, $1 \leqslant i \leqslant s$ and $\{x'_j\}$, $1 \leqslant j \leqslant s'$ be two sets of gridpoints points on $[V_{\min}, V_{\max}]$. If the function N is represented on grid x as $[N_1, \ldots, N_s]^{\mathrm{T}}$ then a representation on the grid x' is given by interpolation:

$$\begin{bmatrix} N'_1 \\ \vdots \\ N'_{s'} \end{bmatrix} = \left[\phi_i(x'_j)\right]^{\mathrm{T}}_{1\leqslant i\leqslant s, 1\leqslant j\leqslant s'} \cdot \begin{bmatrix} N_1 \\ \vdots \\ N_s \end{bmatrix} = T^{x,x'} \cdot \begin{bmatrix} N_1 \\ \vdots \\ N_s \end{bmatrix},$$

where ϕ_i are the basis piecewise-polynomials or spectral polynomials associated with the points $\{x_i\}$.

This interpolation allows us to use a finer grid for growth and a coarser grid for coagulation. This also allows to combine a logarithmic grid for coagulation and a linear grid for growth. The method can be formulated on the fine grid as

$$\left(A - \frac{\Delta t}{2} A \cdot T^{\mathrm{up}} \cdot J^{\mathrm{coag}}\left(T^{\mathrm{down}} n\left(t^k\right)\right) \cdot T^{\mathrm{down}} - \frac{\Delta t}{2} G\right) n\left(t^{k+1}\right) = \left(A + \frac{\Delta t}{2} G\right) n\left(t^k\right),$$

where T^{down} and T^{up} are the transformation matrices from fine to coarse and from coarse to fine (it is easy to see that coagulation is solved on the coarse grid, and the solution extended to the fine grid).

The results displayed in Fig. 4 are obtained using fourth order piecewise polynomial elements (in logarithmic coordinate) with 49 gridpoints for growth and 9 gridpoints for coagulation. The reference solution is well reproduced.

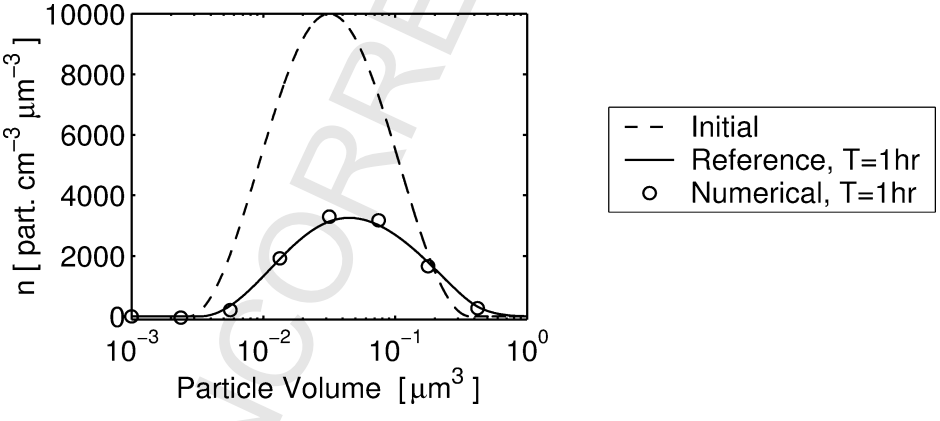

Fig. 4. The coupled coagulation-growth solutions at $t_{\mathrm{final}} = 1$ hour for test problem III. The numerical solution is obtained using fourth order elements on a combined grid with $s = 49$ for growth and $s = 9$ for coagulation.

UNCORRECTED PROOF

A note on conservation properties. The exact solution of the dynamics equation preserves the total number of particles during growth

$$N_{\text{tot}}(t) = \int_0^\infty n(v,t)\,\mathrm{d}v,$$

and the total volume of particles during coagulation

$$V_{\text{tot}}(t) = \int_0^\infty vn(v,t)\,\mathrm{d}v.$$

Exact conservation of the quantities by the numerical distribution is a desirable property (see, e.g., the semi-implicit method [10]). The methods proposed in the framework are not conservative, i.e., they do not exactly conserve these total quantities, and are not positive definite, i.e., they do not guarantee a nonnegative numerical distribution. In Fig. 5 we show the relative differences between the initial and the final total number of particles during growth and the relative differences between the initial and the final

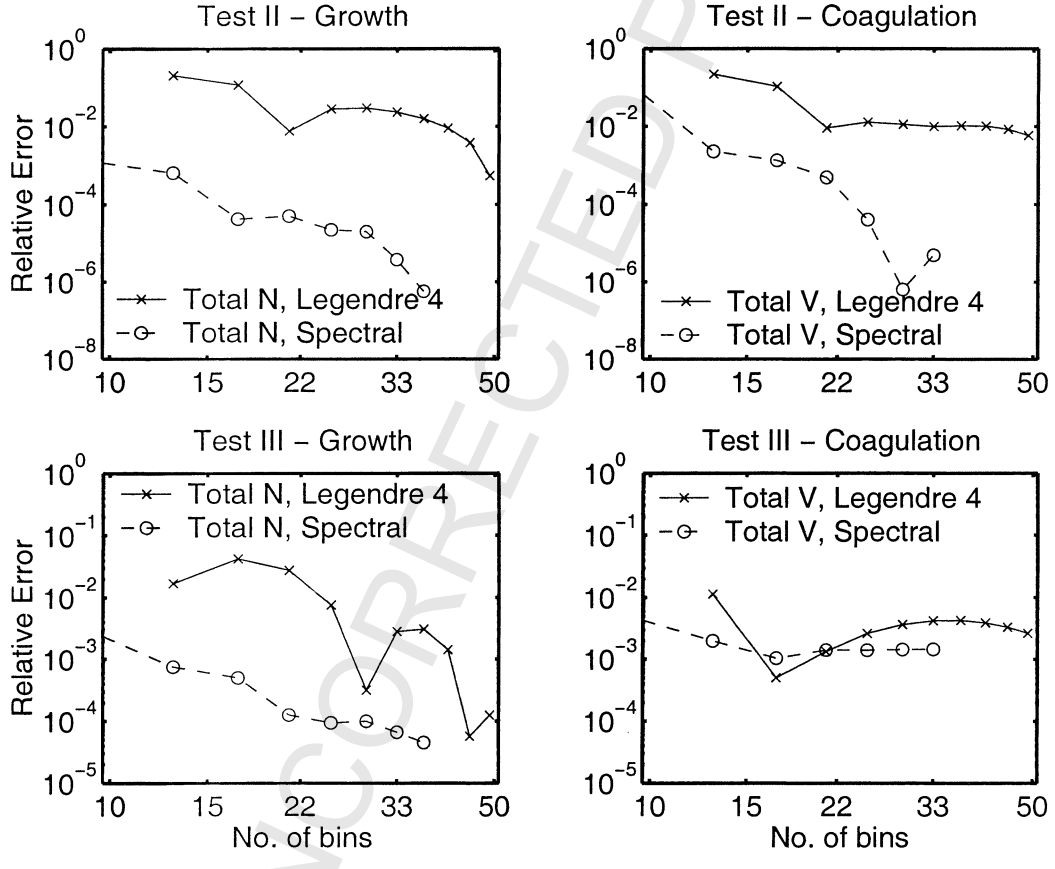

Fig. 5. The relative differences between the initial and the final total number of particles during growth and between the initial and the final total volume of particles during coagulation for test problems II and III.

UNCORRECTED PROOF

Table 2
RMS errors for different timesteps and methods for test problem III. C and G stand for coagulation and growth, respectively

Δt	Spectral discretization					
	C			G		
	1 sec	300 sec	1800 sec	1 sec	300 sec	1800 sec
s = 13	6.31e–3	6.31e–3	6.31e–3	1.70e–2	1.70e–2	1.59e–2
s = 33	2.65e–4	2.65e–4	2.70e–4	9.00e–3	8.63e–3	6.07e-3
Δt	Fourth order Lagrange discretization					
	C			G		
	1 sec	300 sec	1800 sec	1 sec	300 sec	1800 sec
s = 13	6.46e–2	6.44e–2	6.39e–2	1.61e–2	1.60e–2	1.65e–2
s = 33	3.72e–3	3.71e–3	4.06e–3	5.97e–4	5.98e–4	6.05e–4

total volume of particles during coagulation. The total quantities were taken to be the integrals of the fourth order piecewise polynomial interpolant, and of the spectral interpolant respectively. Results are shown for test cases II and III which use logarithmic coordinates. We see the invariants are not exactly preserved, but rather they are preserved within the accuracy of the numerical solution. Exact conservation of invariants may offer additional stability of the solution at very large timesteps.

A note on time steps. The numerical experiments were repeated with much larger time steps (up to $\Delta t = 1800$ s). In Table 2 final solution errors are shown for test problem III under different discretizations and different timesteps; very large time steps could be used without visibly impacting the total accuracy. In general we expect that the growth results will be more sensitive to large timesteps than the coagulation results. In practice one should use a variable time step formula to keep the time discretization error under a given threshold.

8. Conclusions and future work

Aerosols are becoming an important topic in air pollution modeling. For a correct representation of particles in the atmosphere one needs to accurately solve for the size distribution of particle populations.

In this work we developed a general framework for the discretization of aerosol dynamics equations using projection methods, which include Galerkin and collocation approaches. The resulting semidiscrete system is bilinear and can be solved by the time-stepping method of choice; one possible such method is discussed, based on a second order linearly-implicit formula. Although the formulation is given in terms of number densities and single-component particles, it can be directly extended to volume, surface and mass densities, as well as to multiple-component aerosols.

To exemplify the use of the framework we considered a spectral discretization as well as piecewise-polynomial discretizations with linear, quadratic, and fourth order elements. The collocation approach was used for coagulation (all cases) and for growth with spectral elements; the Galerkin approach was used for growth with piecewise polynomial elements. Three test problems were employed. The first two test problems solve a smooth (exponential) profile in linear and logarithmic formulations respectively.

UNCORRECTED PROOF

The third problem considers a cosine hill profile "living" in a finite volume interval and is formulated in logarithmic coordinates.

In linear coordinates the numerical solutions display excellent accuracy. The convergence orders at node points for piecewise polynomial elements are one order better than those predicted by a direct theory; spectral elements show spectral convergence. In logarithmic coordinates (preferred by environmental modelers) good solutions can be obtained for the coagulation equation with a small number of bins ($s \approx 10$); but for accurate growth solutions more gridpoints are needed. A mixed solution is proposed to solve growth on a fine grid and coagulation on a coarse grid. Lower accuracy is generally observed in logarithmic coordinates, although the numerical solutions reproduce well the reference solutions. A more detailed analysis is needed to explain the lower convergence orders observed in the logarithmic formulation.

Future work will focus on developing practical methods within the framework formulation. This involves the identification of suitable families of basis and test functions that are able to resolve the dynamics with a modest number of bins. It is desirable that the invariants of the aerosol dynamics equations are preserved by the numerical scheme (e.g., total volume and total mass are preserved during coagulation and total number during growth). Accurate and robust solutions of the growth equation require some form of upwinding; upwind Petrov–Galerkin and discontinuous Galerkin formulations are currently under investigation.

The main disadvantage of the framework formulation seems to be the computational expense associated with the coagulation tensors B and C as well as the matrices A and G. In the naive approach (where all entries are computed) the cost of the tensors scales with the cube of the number of bins. Fortunately these tensors and matrices are computed once and can be subsequently reused for long time intervals, and possibly for multiple grid points in three-dimensional simulations. The tensors and the matrices are very sparse. A key feature of a good implementation is to predict the sparsity structure and to compute only those entries known to be nonzero. Future work will focus on providing sparse efficient implementations for methods formulated within the framework.

The present numerical tests do not present cpu times, as an efficient sparse implementation is not yet available. Preliminary timings of our matlab implementation (on a Pentium III, 1 GHz machine) for solving the coagulation in the second test problem with $s = 13$ bins, timestep 10 seconds, gives the following cpu times: the semi-implicit method 21 seconds (error 2.1e–2); the spectral method needs 17 seconds for computing the tensors and 6 seconds for the integration (error 6.4e–2); and the piecewise linear polynomials need 80 seconds to assemble the tensors and 6 seconds to integrate (error 4.8e–2).

In a complete aerosol module the cpu time is dominated by the solution of aqueous chemistry and chemical equilibria; the time needed to solve the dynamics is (usually) a relatively small fraction. Thus the main concern is to provide good accuracy with a small number of bins. The practical methods built within the framework will be tested on multiple component particles and on coupled aerosol dynamics and chemistry models.

Acknowledgements

This work was supported by NSF CAREER award ACI-0093139. The authors thank Mark Jacobson for making available his implementation of the semi-implicit method. We also thank the anonymous referees for their comments which helped improve this paper.

UNCORRECTED PROOF

ARTICLE IN PRESS

S0168-9274(02)00251-9/FLA AID:1427 Vol.●●●(●●●)
ELSGMLTM(APNUM):m2 2003/01/03 Prn:7/01/2003; 13:01
anm1427
P.23 (1-23)
by:violeta p. 23

References

[1] K.E. Atkinson, The Numerical Solution of Integral Equations of the Second Kind, Cambridge University Press, Cambridge, 1997.
[2] F.S. Binkowski, U. Shankar, The regional particulate matter model: 1. Model description and preliminary results, J. Geophys. Res. 100 (1995) 26, 191–206, 209.
Uncited [3] A. Bott, A positive definite advection scheme obtained by nonlinear renormalization of the advection fluxes, Monthly Weather Rev. 117 (1989) 1006–1115.
[4] S. Dhaniyala, A. Wexler, Numerical schemes to model condensation and evaporation of aerosols, Atmos. Environ. 30 (1996) 919–928.
[5] F.M. Gelbard, J.H. Seinfeld, Coagulation and growth of a multicomponent aerosol, J. Colloid Interface Sci. 63 (3) (1978) 472–479.
[6] F.M. Gelbard, J.H. Seinfeld, Numerical solution of the dynamic equation for particulate systems, J. Comput. Phys. 28 (1978) 357–375.
[7] F.M. Gelbard, J.H. Seinfeld, Simulation of multicomponent aerosol dynamics, J. Colloid Interface Sci. 78 (2) (1980) 485–501.
[8] M.Z. Jacobson, Development and application of a new air pollution modeling system—II. Aerosol module structure and design, Atmos. Environ. 31 (2) (1997) 131–144.
[9] M.Z. Jacobson, Numerical techniques to solve condensational and dissolutional growth equations when growth is coupled to reversible reactions, Aerosol Sci. Technol. 27 (1997) 491–498.
[10] M.Z. Jacobson, Fundamentals of Atmospheric Modeling, Cambridge University Press, Cambridge, 1999.
[11] C. Johnson, Numerical Solution of Partial Differential Equations by the Finite Element Method, Cambridge University Press, Cambridge, 1987.
[12] Y.P. Kim, J.H. Seinfeld, Simulation of multicomponent aerosol condensation by the moving sectional method, J. Colloid Interface Sci. 135 (1) (1990) 185–199.
[13] F.W. Lurmann, A.S. Wexler, S.N. Pandis, S. Musara, N. Kumar, J.H. Seinfeld, Modeling urban and regional aerosols—ii. Application to California's south coast air basin, Atmos. Environ. 31 (1997) 2695–2715.
[14] A.A. Lushnikov, Evolution of coagulating systems iii. Coagulating mixtures, J. Colloid Interface Sci. 54 (1) (1976) 94–101.
[15] Z. Meng, D. Dabdub, J.H. Seinfeld, Size-resolved and chemically resolved model of atmospheric aerosol dynamics, J. Geophys. Res. 103 (D3) (1998) 3419–3435.
[16] K. Nguyen, D. Dabdub, Semi-Lagrangian flux sheme for the solution of the aerosol condensation/evaporation equation, Aerosol Sci. Technol. (2002), in press.
Uncited [17] M. Phadnis, G.R. Carmichael, Transport and distribution of primary and secondary non-methane hydrocarbons in east Asia under continental outflow conditions, J. Geophys. Res. (1999), in press.
[18] C. Pilinis, Derivation and numerical solution of the species mass distribution equation for multicomponent particulate systems, Atmos. Environ. A 24 (7) (1990) 1923–1928.
[19] J.H. Seinfeld, S.N. Pandis, Atmospheric Chemistry and Physics. From Air Pollution to Climate Change, Wiley, New York, 1997.
Uncited [20] C.H. Song, G.R. Carmichael, Partitioning of hno3 modulated by alkaline aerosol particles, J. Geophys. Res. (1999), in review.
Uncited [21] C.H. Song, G.R. Carmichael, S.Y. Cho, An alternative way to couple kinetic (non-equilibrium/condensation/evaporation) process with thermodynamic equilibrium relationships, Atmos. Environ. (1999), to be submitted.
[22] L.N. Trefethen, Spectral methods in Matlab, SIAM Software, Environments, Tools Series, 2000.
[23] R.P. Turco, P. Hamil, O.B. Toon, R.C. Whitten, C.S. Kiang, The NASA—Ames Research Center stratospheric aerosol model: I. Physical processes and computational analogs, NASA Technical Publication, TP 1362, 1979.
[24] H. Tsang, J.M. Hippe, Asymptotic behavior of aerosol growth in the free molecule regime, Aerosol Sci. Technol. 8 (1988) 265–278.
[25] Y. Zhang, J.H. Seinfeld, M.Z. Jacobson, F.S. Binkowski, Simulation of aerosol dynamics: A comparative review of algorithms used in air quality models, Aerosol Sci. Technol. 31 (1999) 487–514.
[26] A. Wexler, S. Lurmann, J. Seinfeld, Modeling urban and regional aerosols I. Model development, Atmos. Environ. 28 (3) (1994) 531–546.

UNCORRECTED PROOF